Mechanisms of neuronal chloride accumulation in intact mouse olfactory epithelium

William T. Nickell, Nancy K. Kleene and Steven J. Kleene

Department of Cell and Cancer Biology, University of Cincinnati, Cincinnati, OH 45267, USA

When olfactory receptor neurons respond to odours, a depolarizing Cl^- efflux is a substantial part of the response. This requires that the resting neuron accumulate Cl^- against an electrochemical gradient. In isolated olfactory receptor neurons, the Na^+–K^+–$2Cl^-$ cotransporter NKCC1 is essential for Cl^- accumulation. However, in intact epithelium, a robust electrical olfactory response persists in mice lacking NKCC1. This response is largely due to a neuronal Cl^- efflux. It thus appears that NKCC1 is an important part of a more complex system of Cl^- accumulation. To identify the remaining transport proteins, we first screened by RT-PCR for 21 Cl^- transporters in mouse nasal tissue containing olfactory mucosa. For most of the Cl^- transporters, the presence of mRNA was demonstrated. We also investigated the effects of pharmacological block or genetic ablation of Cl^- transporters on the olfactory field potential, the electroolfactogram (EOG). Mice lacking the common Cl^-/HCO_3^- exchanger AE2 had normal EOGs. Block of NKCC cotransport with bumetanide reduced the EOG in epithelia from wild-type mice but had no effect in mice lacking NKCC1. Hydrochlorothiazide, a blocker of the Na^+–Cl^- cotransporter, had only a small effect. DIDS, a blocker of some KCC cotransporters and Cl^-/HCO_3^- exchangers, reduced the EOG in epithelia from both wild-type and *NKCC1* knockout mice. A combination of bumetanide and DIDS decreased the response more than either drug alone. However, no combination of drugs completely abolished the Cl^- component of the response. These results support the involvement of both NKCC1 and one or more DIDS-sensitive transporters in Cl^- accumulation in olfactory receptor neurons.

(Resubmitted 19 March 2007; accepted after revision 25 July 2007; first published online 26 July 2007)
Corresponding author S. J. Kleene: Department of Cell and Cancer Biology, University of Cincinnati, PO Box 670667, Cincinnati, OH 45267, USA. Email: steve@syrano.acb.uc.edu

In most vertebrates, transduction of an odour stimulus into a receptor current occurs on the cilia of the olfactory receptor neurons (ORNs) (Schild & Restrepo, 1998; Frings, 2001). A Ca^{2+}-activated Cl^- current plays a central role in this transduction. Binding of an odourant to the ciliary membrane of an ORN activates a G-protein-coupled cascade that activates an adenylate cyclase (Schild & Restrepo, 1998; Frings, 2001). The cAMP produced gates the first of two transducing channels, the cyclic-nucleotide-gated (CNG) channels (Nakamura & Gold, 1987). Ca^{2+} entering through the CNG channels then gates the second of the transducing channels, the Ca^{2+}-activated Cl^- channels (Kurahashi & Yau, 1993; Kleene, 1993; Lowe & Gold, 1993). In isolated mouse ORNs, the resulting Cl^- current accounts for about 90% of the transduction current (Boccaccio & Menini, 2007). This Cl^- current is conserved throughout the vertebrates (Schild & Restrepo, 1998) and serves to amplify the olfactory response (Kurahashi & Yau, 1993; Kleene, 1993; Lowe & Gold, 1993). It may also insulate the olfactory response against changes in the environment of the transduction apparatus, which necessarily contacts the external world (Kleene & Pun, 1996).

In isolated ORNs held at resting potential, the Cl^- current is usually inward (Kurahashi & Yau, 1993; Zhainazarov & Ache, 1995) and thus tends to depolarize the neuron. This requires that the resting neuron accumulate Cl^- against an electrochemical gradient. The environment of the neuron *in vivo* is much more complex (Fig. 1). In the olfactory epithelium, the neuronal cilia are surrounded by mucus generated by the Bowman's glands and sustentacular cells (Farbman, 1992). The neuronal cell bodies are in a different extracellular compartment and are surrounded by sustentacular cells. Finally, the neuronal axons, as well as the Bowman's glands and basal feet of the sustentacular cells, sit in or near a well-vascularized lamina propria. In intact epithelium, it has been possible to estimate the electrochemical potential for Cl^- near the

This paper has online supplemental material.

 DOI: 10.1113/jphysiol.2007.129601

sensory ending with Cl^--sensitive dyes (Kaneko *et al.* 2004) or energy-dispersive X-ray microanalysis (Reuter *et al.* 1998). Both studies suggest a Cl^- gradient that would cause depolarization.

In most cells, Cl^- homeostasis depends on transporters that allow coupled fluxes of Cl^- and other ions to cross the plasma membrane. In the olfactory system, NKCC1, a Na^+–K^+–$2Cl^-$ cotransporter, plays an important role in neuronal Cl^- accumulation. Pharmacological block or genetic removal of NKCC1 in isolated mouse ORNs virtually abolishes odour-induced Cl^- currents (Reisert *et al.* 2005). However, in intact mouse epithelium, the odour-induced field potential is only modestly reduced in mice lacking NKCC1 (Nickell *et al.* 2006). The remaining field potential in *NKCC1* knockout (KO) mice is largely Cl^- dependent; it is greatly reduced by the Cl^- channel blocker niflumic acid (Nickell *et al.* 2006). These results provide strong evidence that, in intact epithelium, transporters in addition to NKCC1 contribute to neuronal Cl^- accumulation.

The known Cl^- transporters belong to three gene families: Slc4a, Slc12a and Slc26a (Table 1). From an operational standpoint, most of these transporters can also be grouped into four functional classes according to ionic selectivity and pharmacology. The first pharmacological class consists of NKCC1 and NKCC2, which cotransport one Na^+, one K^+ and two Cl^- ions and can be blocked with bumetanide or furosemide (Payne *et al.* 2003; Hebert *et al.* 2004; Gamba, 2005). A second class contains a single protein, NCC, which cotransports one Na^+ and one Cl^- and is blocked by thiazides, including hydrochlorothiazide (Stokes, 1984; Payne *et al.* 2003; Gamba, 2005). A third class exchanges one HCO_3^- for one Cl^-. Some members of this class also exchange Cl^- for other anions, including hydroxide, iodide and formate (Mount & Romero, 2004; Romero *et al.* 2004). DIDS (4,4′diisothiocyanatostilbene-2,2′-disulphonic acid) blocks transport by many Cl^-/HCO_3^- exchangers, including AE1 (Kietz *et al.* 1991), AE2 (Lee *et al.* 1991), AE3 (Lee *et al.* 1991), AE4 (Ko *et al.* 2002; but see also Tsuganezawa *et al.* 2001), PAT1 (Wang *et al.* 2002), SUT2 (Petrovic *et al.* 2003) and Slc26a9 (Xu *et al.* 2005). DIDS inhibition of the Cl^-/HCO_3^- exchangers DRA (Melvin *et al.* 1999; Wheat *et al.* 2000) and pendrin (Soleimani *et al.* 2001; Dossena *et al.* 2006) is uncertain. Transporters in these three classes typically cause accumulation of Cl^- (see Table 1 for references). A fourth class, KCC, cotransports K^+ and Cl^- and can be blocked with DIDS or furosemide (Delpire & Lauf, 1992; Payne, 1997; Mercado *et al.* 2000). The KCC1–4 proteins belong to this class. KCC most often causes extrusion of Cl^- (Payne *et al.* 2003). The classification of the remaining possible Cl^- transporters is less clear: the Slc4a family member NCBE does not cause accumulation of Cl^- (Wang *et al.* 2000), and transporters CCC9, CIP1, TAT1 and Slc26a11 have functions that are not yet well defined (see Table 1 for references).

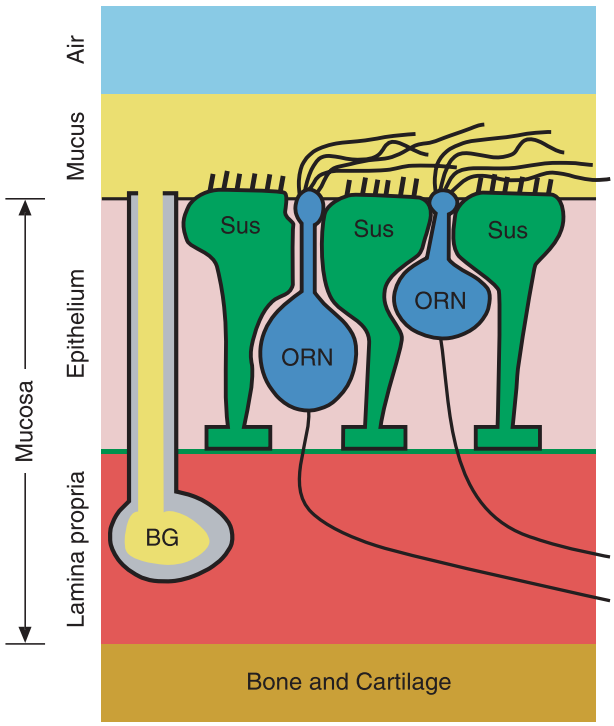

Figure 1. Cartoon diagram of major cell types of the olfactory mucosa *in vivo*
The cilia of the Cl^--accumulating ORNs are exposed to mucus. The mucus is generated by Bowman's glands (BG) and sustentacular cells (Sus) (Farbman, 1992). The ORN cell bodies sit in an extracellular space containing basal cells (not shown) and sustentacular cells. The Bowman's glands, ORN axons and basal feet of the sustentacular cells sit near or in a well-vascularized lamina propria. The ORN-containing olfactory epithelium and its underlying lamina propria comprise the olfactory mucosa.

In intact olfactory epithelium, we have investigated which Cl^- transporters in addition to NKCC1 allow ORNs to accumulate Cl^-. We first used the reverse transcriptase-polymerase chain reaction (RT-PCR) to determine which Cl^- transporters are expressed in nasal tissue containing olfactory mucosa. We then investigated how pharmacological block or genetic removal of Cl^- transporters affects the electroolfactogram (EOG), the odour-induced field potential measured at the surface of the epithelium. The EOG arises primarily from the receptor potentials of the ORNs (Ottoson, 1956; Scott & Scott-Johnson, 2002).

Methods

RT-PCR

To obtain RNA, adult mice (strain C57Bl6/129) were exposed to rising concentrations of CO_2 and then decapitated in accordance with the University of

Table 1. Cl transporters

Family	Gene	Alias	Distribution	Ions	Cl^- Influx(I) or efflux(E)	References
Slc4a anion exchangers	***Slc4a1***	***kAE1***	kidney	Cl^-/HCO_3^-	I	Alper *et al.* 2002; Romero *et al.* 2004
	Slc4a1	***eAE1***	erythrocyte	Cl^-/HCO_3^-	I	
	Slc4a2	***AE2***	widespread	Cl^-/HCO_3^-	I	
	Slc4a3	***AE3***	brain, heart	Cl^-/HCO_3^-	I	
	Slc4a9	***AE4***	kidney, stomach	Cl^-/HCO_3^-	I	Tsuganezawa *et al.* 2001; Ko *et al.* 2002; Xu *et al.* 2003
	Slc4a10	***NCBE***	brain, ileum, kidney	$Cl^-/Na^+ + 2HCO_3^-$	E	Wang *et al.* 2000
Slc12a electro neutral, cation–coupled cotransporter	***Slc12a1***	***NKCC2***	kidney	$Na^+ + K^+ + 2Cl^-$	I	Payne *et al.* 2003
	Slc12a2	***NKCC1***	widespread	$Na^+ + K^+ + 2Cl^-$	I	
	Slc12a3	***NCC***	kidney	$Na^+ + Cl^-$	I	
	Slc12a4	***KCC1***	widespread	$K^+ + Cl^-$	E	
	Slc12a5	***KCC2***	neuron-specific (brain)	$K^+ + Cl^-$	E, I	Payne *et al.* 2003; Gamba, 2005
	Slc12a6	***KCC3***	widespread	$K^+ + Cl^-$	E	
	Slc12a7	***KCC4***	widespread	$K^+ + Cl^-$	E	
	Slc12a8	***CCC9***	widespread	?	?	Hebert *et al.* 2004; Gamba, 2005
	Slc12a9	***CIP1***	widespread	?	?	Gamba, 2005
Slc26a	***Slc26a3***	***DRA***	colon, pancreas, trachea	Cl^-/HCO_3^-	I	Greeley *et al.* 2001; Sterling & Casey, 2002; Mount & Romero, 2004
	Slc26a4	***pendrin***	thyroid, inner ear, kidney	Cl^-/HCO_3^-	I	Sterling & Casey, 2002; Mount & Romero, 2004
	Slc26a6	***PAT1***	pancreas, kidney, stomach	Cl^-/HCO_3^-	I	Sterling & Casey, 2002; Wang *et al.* 2002; Mount & Romero, 2004
	Slc26a7	***SUT2***	kidney, stomach	Cl^-/HCO_3^-	I	Sterling & Casey, 2002; Petrovic *et al.* 2003, 2004
	Slc26a8	***TAT1***	testis	Cl^-	?	Lohi *et al.* 2002; Sterling & Casey, 2002
	Slc26a9		lung, stomach	Cl^-/HCO_3^-	I	Sterling & Casey, 2002; Xu *et al.* 2005
	Slc26a11		widespread	Cl^-/HCO_3^-	?	Vincourt *et al.* 2003; Soleimani & Xu, 2006

The genes are classified by sequence homology into three families: Slc4a, Slc12a and Slc26a. Several of the transporters have common names, some of which are listed in the 'Alias' column. The 'Distribution' and 'Ions' columns are not exhaustive. Ions separated by '+' are cotransported; ions separated by '/' are exchanged. The 'Cl^- influx (I) or efflux (E)' column indicates the likely direction of Cl^- transport *in vivo* in the tissues that have been studied.

Cincinnati's Institutional Animal Care and Use Committee protocols and to conform with NIH guidelines. Care was taken to remove the nasal tissue without contamination from the olfactory bulb. Nasal tissue containing olfactory mucosa (hereinafter referred to simply as nasal tissue) was obtained by removing the turbinates and caudal septum. Thus, the sample contained olfactory mucosa with some bone, cartilage and respiratory mucosa. Total RNA was extracted from this and from the positive control tissues with TRIzol Reagent (Invitrogen, Carlsbad, CA, USA). The RNA was treated with DNase (DNA-*free* kit, Ambion, Austin, TX, USA) and reverse transcribed with oligo (dT) primers (RETROscript kit, Ambion; RNase inhibitor, Fisher, Waltham, MA, USA). PCR reactions were run for 30 cycles with a Taq polymerase PCR kit (T-20, GeneChoice, Frederick, MD, USA). RT-PCR reactions were run with 3.7 ng RNA $(\mu l$ RT-PCR reaction$)^{-1}$; this RNA concentration was within the range (1–10 ng RNA μl^{-1}) recommended by the RETROscript protocol. Weak or negative reactions (*kAE1*, *AE4*, *NCBE*, *NKCC2*, *NCC* and *DRA*) were further tested with 15 ng RNA μl^{-1}. Primer sequences, annealing temperatures and references or NCBI

accession numbers are given in the Supplemental material available online (SM-Table 1). Each PCR product crosses at least one intron; as a result, any genomic DNA would yield a significantly longer PCR product than expected. Primer sequences were obtained from the literature (*AE1*) or from M. Soleimani (*DRA*) or chosen using Primer3 software (Rozen & Skaletsky, 2000). For all of the transporters except *AE1* and *CCC9*, the primers were designed to amplify a PCR product that would have the same sequence for all known variants of a given transporter. In such cases, a positive result does not reveal which variants are present. For *AE1*, the primers were designed to differentiate between the two variants, *kAE1* and *eAE1*. For *CCC9*, for which a new variant was recently found (NM_001083902), the primers should amplify PCR products of nearly the same sizes (9 basepair difference) but different sequences for the two variants. There is some evidence that *Slc26a9* has two variants in mouse, but only one sequence is known (Xu *et al.* 2005), so that sequence was used to design primers. In all cases, nasal samples that gave negative results for a given transporter had given positive results for other transporters. PCR products were separated on an agarose gel and stained with ethidium bromide. The PCR product was extracted from the gel (MinElute Gel Extraction Kit, Qiagen, Valencia, CA, USA) and sequenced to confirm the identity of the PCR product. All transporters were sequenced from reactions with the conventional RNA concentration (3.7 ng RNA μl^{-1}) except *AE4*, *NCBE*, *NKCC2* and *NCC*, which were sequenced from reactions with 15 ng RNA μl^{-1}. When a transporter was not found in the nasal tissue, the PCR product from the positive control tissue was sequenced. The sequence of the PCR product was BLASTed against the mouse database to confirm that the selected Cl^- transporter was the only gene with that sequence (NCBI BLASTN, mouse nr/nt database, Altschul *et al.* 1997).

Every PCR reaction was accompanied by a control ('no-transcript') reaction in which water was run in place of RT product to test for contamination of PCR reagents; these controls were always negative. Each transporter was tested with two different nasal samples; the same transporters were detected with both samples with the exception of two weakly detected transporters (*DRA* and an *NCBE* splice variant; see Results). Aerosol tips were used for RNA extraction, DNase treatment and RT-PCR procedures. On the agarose gels, the PCR product for the positive control tissue was at least one well away from the PCR product for the nasal tissue. Lack of contamination is supported by the finding that both nasal samples were negative by RT-PCR for genes expressed in kidney (*kAE1*, Fig. 2*A*), cerebellum (*ZIC2*, NM_009574, data not shown) and stomach (*GKN1*, NM_025466, data not shown). For *NKCC2*, additional nasal tissue (23-day-old mice, inbred FVBN strain) was acquired and processed in conjunction with a blank sample through the RNA extraction, DNase treatment and RT-PCR procedure. The nasal sample was positive for *NKCC2*, as shown by sequencing, while the control was negative.

Electroolfactogram

We measured the electroolfactogram (EOG), which is commonly used to quantify the odour-induced potential in mouse olfactory epithelium (Wong *et al.* 2000; Spehr *et al.* 2006; Wang *et al.* 2006). EOGs were recorded in epithelia from $NKCC1^{+/+}$ and $NKCC1^{-/-}$ mice in an inbred FVBN background (Flagella *et al.* 1999) or from $AE2^{+/+}$ and $AE2^{-/-}$ mice in a mixed 126S6/SvEv and Black Swiss background (Gawenis *et al.* 2004). Both knockouts contain null mutations. The genotype of each mouse was determined by PCR of DNA from tail biopsies. Turbinates were exposed and mounted as previously described (Nickell *et al.* 2006). The tissue was continuously perfused by a gravity flow system through a four-input solenoid valve manifold (General Valve, Fairfield, NJ, USA) at 1 ml min^{-1}. Odor stimulation was applied by computer-controlled switching of the valve to odour-containing Ringer solution (a mixture of 10 odourants: 2-heptanone, (*S*)(+)-carvone, isoamyl acetate, anisole, pyridine, benzaldehyde, *n*-hexanoic acid, cineole, *n*-butanol, and ethyl *n*-butyrate, 100 μM each). The valve manifold was mounted near the preparation, and 10 cm of PE20 tubing carried Ringer solution from the common port of the manifold to the preparation. This tubing provided the resistance regulating flow from reservoirs positioned 50 cm above the preparation. The distal end of the tubing was attached to a manipulator and its position was adjusted to produce uniform flow over the turbinates. Dye (fast green, 0.01% w/v) was included in the odour solution to monitor stimulus delivery. One channel of the valve manifold was connected to a solution containing dye but no added odourant. This allowed verification of stimulus delivery without exposing the epithelium to stimulus. The odour-free solution produced very small responses. Procedures were similar to those previously described (Nickell *et al.* 2006). In that study, a picospritzer (General Valve) and a separate stimulus pipette were used to inject the odourant mixture into a continuous stream of Ringer solution.

For each experiment, a mouse was euthanized as described above. The head was hemisected in a midsagittal plane with the blade passing between the septum and the lateral wall. The septum was removed, and recordings were made from the olfactory turbinates, which are located on the lateral wall. Most EOGs were recorded from endoturbinate III (using the nomenclature of Ressler *et al.* 1993). The Ringer solution consisted of (mM): 140 NaCl, 5 KCl, 2 $CaCl_2$, 1 $MgCl_2$, 10 Hepes and 10 glucose, adjusted to pH 7.2 with NaOH. Each epithelium was tested with a single Cl^--transport blocker (or mixture of blockers) and then discarded.

In some experiments a different dissection was used. The mucosa covering the septum was removed from underlying cartilage and bone. The isolated mucosa (about 5 mm × 6 mm) was positioned on a 1 cm^2 square of 105 μm nylon mesh (Small Parts, Miami Lakes, FL, USA) and supported by a silicone base so that it sat at a 45 deg angle. The tissue was held in place by a harp of the kind used to secure brain slices for recording. The elastic strings of the harp were placed on both sides of the platinum wire so that surface tension maintained a constant depth of fluid above the tissue. The nylon mesh was permeable and hydrophilic, allowing a constant flow beneath the tissue. This arrangement ensured drug access to both sides of the mucosa.

The recording electrode was a 20-μm-diameter fire-polished pipette pulled from haematocrit tubing, filled with Ringer solution, and attached to a stable manipulator. The tip was positioned a few microns above the surface of the epithelium, as determined by an increase in electrical resistance and the presence of multiunit activity on touching the epithelium. Electrical signals were amplified by a high-impedance preamplifier (AK-47LN, Metametrics, Cambridge, MA, USA), filtered at 500 Hz and digitized at 2 kHz. Data acquisition and stimulus control were handled by a data-acquisition board (PCI-6024E, National Instruments, Austin, TX, USA) run by Igor Pro 4 software (Wavemetrics, Portland, OR, USA). The preparation was grounded through a 3 M KCl salt bridge. Recordings were done at room temperature (22–25°C).

Hydrochlorothiazide (H2910), bumetanide (B3023) and DIDS (D3514) were purchased from Sigma-Aldrich (St Louis, MO, USA). The concentrations of blockers used in this report were expected to produce almost total inhibition of the targeted Cl^- transporters, based on numerous dose–response studies (see the references in the introduction).

Block of ciliary transduction channels

The effects of bumetanide and DIDS on the CNG and Cl^- transduction channels were measured by patch recording from single olfactory cilia of the grass frog (Kleene, 1993). Frogs were decapitated and doubly pithed without anesthesia in accordance with the University of Cincinnati's Institutional Animal Care and Use Committee protocols and in conformation to NIH guidelines. CNG and Cl^- channels were activated by adding 100 μM cAMP or 300 μM $CaCl_2$, respectively, to the cytoplasmic bath. Slope conductance of the ligand-activated current was measured between −60 and −40 mV. Bumetanide (50 μM) or DIDS (500 μM or 1 mM) was then applied to the extracellular face of the cilium by perfusing the patch pipette. Ten minutes following perfusion, the slope conductance was measured again to determine the extent of channel block.

Analysis of data

For each epithelium, each EOG amplitude was normalized by dividing it by the average of all of the control points. Thus, the mean normalized control value for each epithelium is 1.0. Straight lines shown in the figures are linear regressions determined from the mean values. In most experiments, the EOG amplitude declined slowly with time (e.g. Fig. 3) even in the control condition. Such a decline in the EOG with repeated odour stimulation has been previously reported in frog (Gesteland *et al.* 1965) and rat (Gesteland & Sigwart, 1977). We determined the decrease in EOG amplitude due to pharmacological block in Figs 3 and 5 as follows. Two linear regressions were calculated, one from the control points and one from the data following treatment. The value of each regression line at the time of the first treatment point (35 min in Fig. 3 and 15 min in Fig. 5) was determined. The decrease was figured from the ratio of those two values. In effect, this compares the amplitude immediately following treatment to the predicted value of the control experiment at that same time.

To compare different treatments or populations, we used analysis of variance (ANOVA) using the Mixed Procedure of SAS (SAS Institute, Cary, NC, USA). Significance of differences between individual data points was determined using unpaired *t* tests. Data are reported as mean ± S.E.M.

Results

Many Cl^- transporters are expressed in nasal tissue

Using RT-PCR, mRNA transcripts for 20 of the 21 Cl^- transporters were detected in nasal tissue that contained olfactory mucosa, and the identities of the PCR products were confirmed by sequencing. The remaining transporter, *DRA*, was detected as a weak band; sequencing of that band was not attempted.

With a conventional amount of RNA (3.7 ng RNA (μl RT-PCR reaction)$^{-1}$), mRNA for all transporters except *NKCC2* and *DRA* was detected in mouse nasal tissue (Fig. 2). Sequencing confirmed the identities of the bands; some weak bands (*AE4*, *NCBE NCC*) were sequenced from reactions with a greater amount of RNA (15 ng RNA μl^{-1}). When *NKCC2* was tested with 15 ng RNA μl^{-1}, it was detected (data not shown) and confirmed with sequencing. When *DRA* was tested with 15 ng RNA μl^{-1}, a faint band was detected at the appropriate size (data not shown) in one of two nasal samples. We did not attempt to sequence this band. For *AE1*, the primers were designed to differentiate between the two variants (*kAE1* and *eAE1*). *eAE1* was detected in nasal tissue; *kAE1* was not detected (Fig. 2*A*), even at the higher RNA concentration (data not shown). For *CCC9*, the sequence matched variant 1 (NM_134251) rather than variant 2 (NM_001083902). For

all transporters except *AE1* and *CCC9*, the primers were designed to amplify a PCR product that would have the same sequence for all known variants of a given transporter. In such cases, a positive result does not reveal which variants are present. For *KCC4*, we detected a new mRNA splice variant upon sequencing the PCR product from nasal tissue. The 15 extra bases (AGAGTGGGGAAACCT) are located in the intron that precedes exon 23 (see Discussion). *KCC4* that was sequenced from the positive control tissue (kidney) did not include the extra bases. For *NCBE*, we detected a new mRNA splice variant upon sequencing the PCR product from nasal tissue. The nasal *NCBE* was missing exon 25 (NM_033552) and its band ran faster on the gel than the brightest band from brain tissue (Fig. 2*A*). The sequence we obtained from the brightest band with the brain tissue matched the published sequence (NM_033552). The brain tissue showed a weak band at the same size as the nasal *NCBE* variant; we did not sequence the DNA from that band in brain. At 15 ng RNA μl^{-1}, nasal tissue had a band at the same size as the brightest band from the brain tissue (data not shown); at 3.7 ng RNA μl^{-1}, a weak, similarly positioned band was detected in only one of two nasal samples (data not shown).

To further characterize the Cl^- transport processes underlying olfactory transduction, we studied the

A RT-PCR for the Slc4a chloride transporters

Gene	*Slc4a1*			*Slc4a1*			*Slc4a2*			*Slc4a3*			*Slc4a9*			*Slc4a10*		
Alias	*kAE1*			*eAE1*			*AE2*			*AE3*			*AE4*			*NCBE*		
No. of Known Murine Splice Variants	–			–			5			2			1			1		
Results for Nasal Tissue	−			+			+			+			+			+		
Expected Size (bp)	512			533			569			570			515			345		
Tissue	K	N	NT	Sp	N	NT	Ce	N	NT	B	N	NT	K	N	NT	B	N	NT

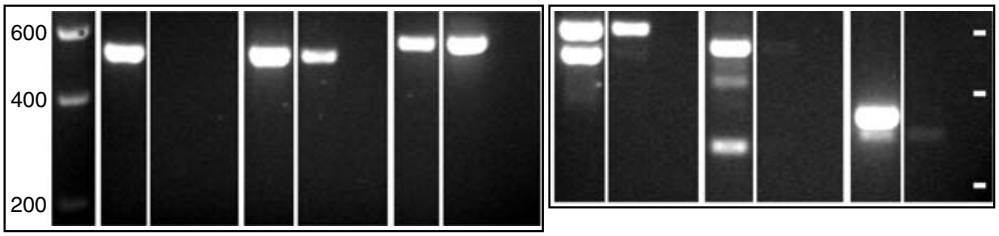

B RT-PCR for the Slc12a1 - Slc12a5 chloride transporters

Gene	*Slc12a1*			*Slc12a2*			*Slc12a3*			*Slc12a4*			*Slc12a5*		
Alias	*NKCC2*			*NKCC1*			*NCC*			*KCC1*			*KCC2*		
No. of Known Murine Splice Variants	6			2			1			1			1		
Results for Nasal Tissue	+[1]			+			+			+			+		
Expected Size (bp)	152			516			521			597			512		
Tissue	K	N	NT	K	N	NT	K	N	NT	K	N	NT	Ce	N	NT

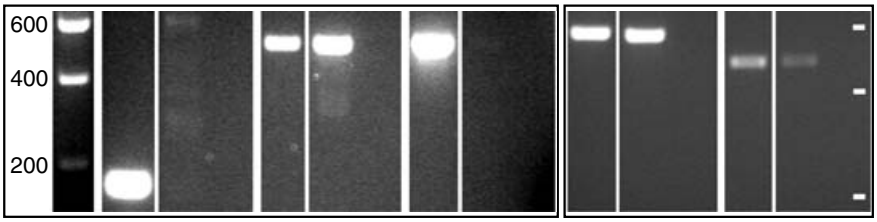

Figure 2. Continued.

olfactory field potential, known as the electroolfactogram (EOG). This potential is measured at the surface of the olfactory epithelium during odour stimulation. The EOG arises from the summated activities of many ORNs near the recording electrode (Ottoson, 1956; Scott & Scott-Johnson, 2002). It is primarily caused by a depolarizing Cl^- current and is thus an indicator of the neuronal Cl^- gradient (Nickell *et al.* 2006). We measured the effects of Cl^- transport inhibitors and genetic ablation of specific transporters on the EOG. The results are described in the following sections.

The EOG survives genetic ablation of NKCC1

For epithelia from wild-type (WT) mice, the mean EOG amplitude was $913 \pm 96\ \mu V$ ($n = 20$). In *NKCC1* knockout

C RT-PCR for the Slc12a6 - Slc12a9 chloride transporters

Gene	*Slc12a6*			*Slc12a7*			*Slc12a8*			*Slc12a9*		
Alias	*KCC3*			*KCC4*			*CCC9*			*CIP1*		
No. of Known Murine Splice Variants	5			1			2			1		
Results for Nasal Tissue	+			+			+			+		
Expected Size (bp)	554			484			591			589		
Tissue	K	N	NT	K	N	NT	Co	N	NT	B	N	NT

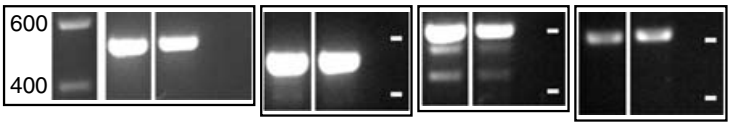

D RT-PCR for the Slc26a chloride transporters

Gene	*Slc26a3*			*Slc26a4*			*Slc26a6*			*Slc26a7*			*Slc26a8*			*Slc26a9*			*Slc26a11*		
Alias	*DRA*			*Pendrin*			*PAT1*			*SUT2*			*TAT1*								
No. of Known Murine Splice Variants	1			1			2			1			1			1			1		
Results for Nasal Tissue	$-^2$			+			+			+			+			+			+		
Expected Size (bp)	497			585			469			593			577			521			587		
Tissue	Co	N	NT	K	N	NT	SI	N	NT	St	N	NT	T	N	NT	St	N	NT	K	N	NT

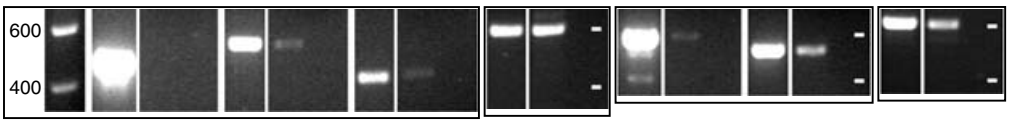

Figure 2. mRNA for Cl^- transporters in nasal tissue containing olfactory mucosa assayed by RT-PCR
A, RT-PCR for the Slc4a Cl^- transporters. *B*, RT-PCR for the Slc12a1–Slc12a5 Cl^- transporters. *C*, RT-PCR for the Slc12a6–Slc12a9 Cl^- transporters. *D*, RT-PCR for the Slc26a Cl^- transporters. The expression of genes for 21 Cl^- transporters was tested. The images of gels show the results of RT-PCR reactions with a conventional RNA concentration (3.7 ng RNA μl^{-1}). For all of the transporters except *AE1* and *CCC9 (*see Methods), the primers were designed to amplify a PCR product that would have the same sequence for all known variants of a given transporter. In the row 'Results for Nasal Tissue', '+' (without a superscript) indicates that one or more of the variants for the Cl^- transporter was detected with a conventional RNA concentration and confirmed with sequencing; '−' (without a superscript) indicates that *kAE1* was not detected. '$+^1$' indicates that while *NKCC2* was negative at 3.7 ng RNA μl^{-1}, it was detected (data not shown) and confirmed with sequencing with 15 ng RNA μl^{-1}. '$-^2$' indicates that *DRA* was negative at 3.7 ng RNA μl^{-1} but had a weak band (data not shown), which was not sequenced, at 15 ng RNA μl^{-1}. For *NCBE* and *KCC4*, the number of variants shown refers to the one variant that was known prior to the present study. For each transporter, nasal tissue (N), a 'no-transcript' (NT) control, and the appropriate positive control tissue (K, kidney; Sp, spleen; Ce, cerebellum; B, brain; Co, colon; SI, small intestine; St, stomach; and T, testis) were tested. In the first gel image of each section of the figure (*A*, *B*, *C* or *D*), the leftmost lane is a calibration lane; the values are in basepairs. Thereafter, the calibration marks are indicated by white dashes in the rightmost lane of each gel. The values for the calibration marks are the same for all gels in a section. A box around multiple lanes indicates that the lanes were part of the same gel. bp, basepair.

(KO) mice, the mean was $387 \pm 66\ \mu V$ ($n = 15$), which is 57% smaller than the mean response in the WT. The difference is highly significant ($P < 0.001$).

In a previous study (Nickell *et al.* 2006), we reported that the EOG amplitude in *NKCC1* KO mice was 39% smaller than in WT mice. The mean EOG amplitudes were smaller in that study: $438 \pm 65\ \mu V$ ($n = 7$) in WT mice and $268 \pm 19\ \mu V$ ($n = 7$) in *NKCC1* KO mice. There were two methodological differences between the two studies. The present study used a slightly more precise method of stimulus delivery (see Methods) and also used older mice. Mice used in the first study were 19–52 days old. The means shown above for the present study are from WT mice of average age 87 ± 5 days ($n = 20$, range 50–113 days) and KO mice of average age 111 ± 11 days ($n = 15$, range 49–114 days).

Treatment with bumetanide simulates the absence of NKCC1

We also examined the role of NKCC1 in WT mice by blocking the transporter with bumetanide. The other possible target of bumetanide, NKCC2, was detected in nasal tissue by RT-PCR (data not shown) in this study but has not been previously detected in olfactory tissue (Kaneko *et al.* 2004; Reisert *et al.* 2005). We expected that a WT epithelium treated with bumetanide would be similar to an epithelium from an *NKCC1* KO mouse, and that bumetanide should have little effect in mice lacking NKCC1. These predictions were verified.

In epithelia from WT and *NKCC1* KO mice, we recorded the EOG response amplitudes before and after application of bumetanide (Fig. 3). Control responses were taken at 5 min intervals for 30 min. The control response amplitude declined 0.8% min^{-1} and 1.1% min^{-1} in WT and KO epithelia, respectively. Immediately after the final control response, 50 μM bumetanide was added to the perfusing solution and responses were taken for an additional 30 min. In epithelia from WT mice, the EOG amplitude decreased by 32% immediately after application of bumetanide. In epithelium from *NKCC1* KO mice, the response increased 4%. In the WT mice, the decrease was highly significant ($P < 0.0001$); in the KO mice, the difference was not significant ($P < 0.5$). Since bumetanide did not affect the EOG response in *NKCC1* KO mice, it can be considered a specific blocker of NKCC1 in this system. During continuous application of bumetanide, responses in both KO and WT continued to decline at rates near the control rates.

Block of additional Cl^- transporters further reduces the EOG amplitude but does not abolish the response

In epithelia from WT mice, we attempted to simultaneously block all four classes of Cl^- transporter. Epithelia were treated with an 'All Block' mixture containing 50 μM bumetanide (which blocks NKCC1), 200 μM hydrochlorothiazide (which blocks NCC), and 500 μM DIDS (which blocks many of the KCC cotransporters and Cl^-/HCO_3^- exchangers).

The All Block mixture reduced the response amplitude within 5 min of drug application (Fig. 4*A*). There was no further reduction at 10 min following drug exposure. On average, the All Block treatment reduced the EOG amplitude by 63% (determined by comparing the average of the 3 control responses to the average of the 2 following treatment). Following this treatment, niflumic acid (300 μM) was added to the perfusing solution (Fig. 4*B*). Niflumic acid reduced the response amplitude by $94 \pm 1\%$ (compared with the mean control value) after 5 min of exposure and by $99 \pm 1\%$ after 10 min ($n = 5$). Niflumic acid blocks the ciliary Cl^- channels that open during the odour response (Kleene, 1993; Lowe & Gold, 1993).

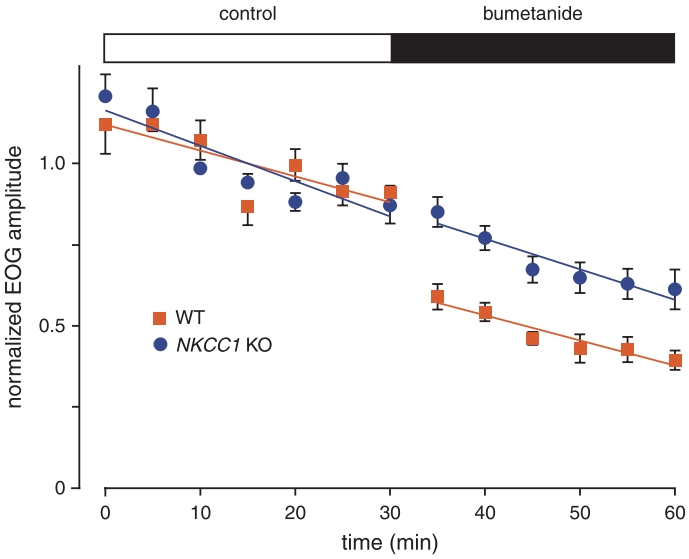

Figure 3. Block of the NKCC1 cotransporter by bumetanide reduces the EOG amplitude in WT but not in *NKCC1* KO mice
The concentration of bumetanide was 50 μM. Mice were 45–86 days old. The WT series used 6 epithelia from 4 mice; the KO series used 4 epithelia from 2 mice.

The All Block mixture reduced the response more than did bumetanide alone. To determine whether the additional reduction was caused by hydrochlorothiazide or by DIDS, we next tested each blocker separately.

Block of the NCC cotransporter only slightly reduces the EOG amplitude

NCC is expressed in olfactory tissue of rat (Kaneko *et al.* 2004) and mouse (Fig. 2*B*). We tested the effect of 200 μM hydrochlorothiazide, which blocks NCC, on the EOG. If NCC contributes to neuronal accumulation of Cl^-, then hydrochlorothiazide should decrease the EOG amplitude. If NCC and NKCC1 are the *only* transporters accumulating Cl^-, then hydrochlorothiazide might virtually eliminate the EOG in *NKCC1* KO mice but not in WT mice. The combined WT and KO responses (Fig. 5*A*) were decreased 11% after application of hydrochlorothiazide. This decrease was weakly significant ($P < 0.05$). However, the difference between the two genotypes was not significant ($P < 0.07$). This result suggests that NCC plays a limited role in Cl^- accumulation.

Treatment with DIDS reduces the EOG amplitude in both WT and *NKCC1* KO epithelia

As described above, DIDS blocks many KCC cotransporters and Cl^-/HCO_3^- exchangers. If a DIDS-sensitive transporter functions alongside NKCC1, then block of the DIDS-sensitive transporter should reduce the EOG amplitude. If NKCC1 and a DIDS-sensitive transporter are the *only* transporters accumulating Cl^-, then DIDS might virtually abolish the EOG in the *NKCC1* KO mouse.

As before, EOG amplitudes were measured before and after application of the transport blocker in both WT and *NKCC1* KO epithelia. DIDS (1 mM) decreased the EOG within 5 min of its application (Fig. 5*B*). There was no difference in percentage reduction between the WT and *NKCC1* KO epithelia ($P < 0.2$). When both data sets (WT and KO) were combined, the percentage reduction by DIDS was 42%. This decrease is highly significant ($P < 0.0001$). Thus, DIDS reduces the EOG amplitude but does not abolish the response even in *NKCC1* KO mice.

Niflumic acid (300 μM) was applied to some of the epithelia following the treatment with DIDS. Niflumic acid reduced the response amplitude by $94 \pm 2\%$ (compared with the mean control value) after 5 min of exposure (pooled results from 4 WT and 3 *NKCC1* KO mice). This indicates that an odour-induced Cl^- current persists even following perfusion with DIDS.

Effects of DIDS and bumetanide on the ciliary transduction channels

In principle, the blockers tested could reduce the EOG by blocking the ciliary transduction channels rather than by blocking Cl^- accumulation. The effects of extracellular DIDS and bumetanide on the CNG and Cl^- transduction channels were determined in frog, where it is possible to record from single olfactory cilia. DIDS, which is known to block some Cl^- channels, inhibited the olfactory Cl^- conductance slightly ($8 \pm 4\%$ reduction at 500 μM, $n = 5$; $13 \pm 8\%$ reduction at 1 mM, $n = 8$). Bumetanide

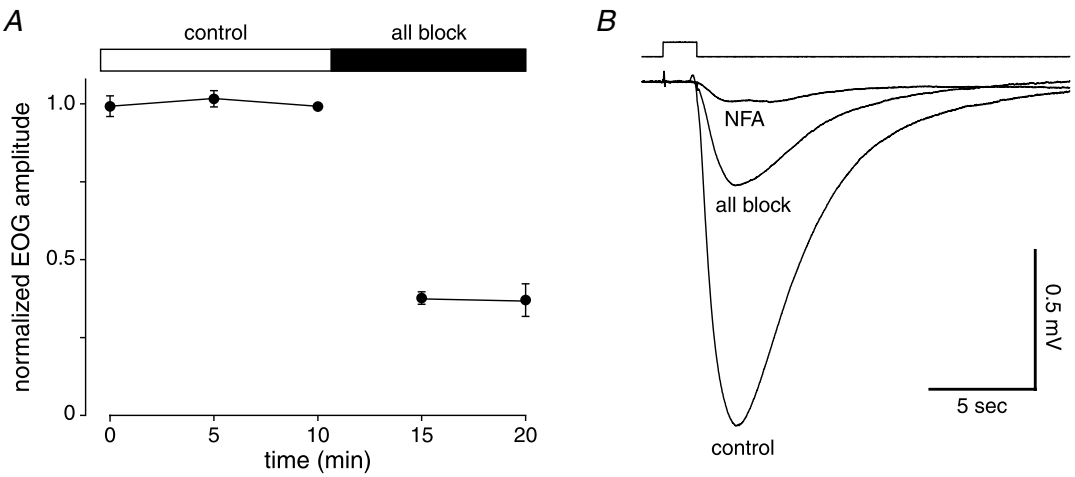

Figure 4. Simultaneous block of multiple Cl^- uptake systems reduces the EOG amplitude but does not abolish the response in WT mice
Mice were all WT, 77–87 days old. Five epithelia from 3 mice were used. *A*, normalized EOG amplitudes before and after application of the All Block mixture of three transport blocking drugs (50 μM bumetanide, 500 μM DIDS and 200 μM hydrochlorothiazide). *B*, example EOG responses recorded in the following order: control; after application of the All Block mixture; and after application of niflumic acid (NFA, 300 μM).

(50 μM) reduced the ciliary Cl^- conductance by $7 \pm 1\%$ ($n = 6$). Neither inhibitor had a significant effect on the CNG conductance ($n = 4$ for bumetanide; $n = 5$ for DIDS).

Mice lacking AE2 have a normal EOG

AE2 is a Cl^-/HCO_3^- exchanger (Alper *et al.* 2002) that has widespread expression including nasal tissue (Shetty *et al.* 2005; and Fig. 2*A*). If NKCC1 and AE2 are solely

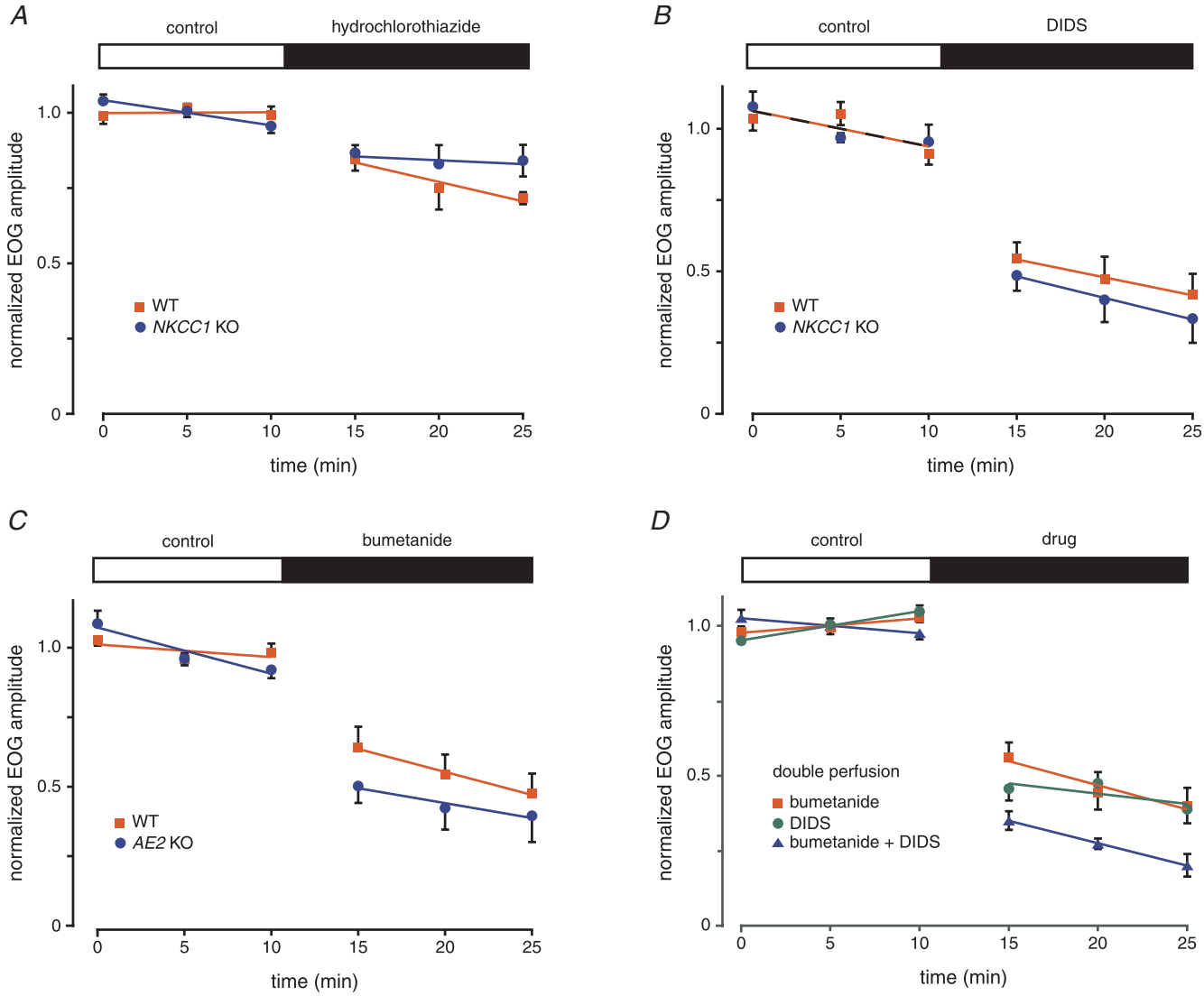

Figure 5. Further pharmacological studies of the EOG in WT and KO mice
A, hydrochlorothiazide, a blocker of the NCC transporter, has only small effects on the EOG amplitude in WT and *NKCC1* KO mice. Hydrochlorothiazide concentration was 200 μM. Mice were 99–103 days old (WT) and 104–176 days old (KO). The WT series used 4 epithelia from 2 mice; the KO series used 6 epithelia from 4 mice. *B*, DIDS reduces the EOG amplitude in both WT and *NKCC1* KO mice. DIDS concentration was 1 mM. Mice were 109–115 days old (WT) and 111–115 days old (KO). For each of the WT and KO series, 5 epithelia from 3 mice were used. *C*, bumetanide reduces the EOG amplitude in both WT and *AE2* KO mice. The bumetanide concentration was 50 μM. Mice were 13–16 days old (WT) and 15–16 days old (KO). *AE2* KO mice do not survive beyond weaning. For the WT series, 6 epithelia from 5 mice were used; for the *AE2* KO series, 7 epithelia from 5 mice were used. *D*, application of bumetanide and DIDS to both surfaces of the mucosa does not eliminate the EOG. Responses are from septal mucosa that was removed from underlying cartilage and mounted on nylon mesh. Bumetanide concentration was 50 μM; DIDS concentration was 500 μM. All mice were adult WT aged 79–80 days (bumetanide only), 106–144 days (DIDS only) or 109–128 days (bumetanide plus DIDS). The first series (bumetanide only) used 5 epithelia from 3 mice; the second series (DIDS only) used 7 epithelia from 4 mice; the third series (bumetanide and DIDS) used 5 epithelia from 3 mice. Residual responses were strongly decreased or abolished by 300 μM niflumic acid (data not shown).

responsible for Cl^- uptake in ORNs, then block of NKCC1 by bumetanide in mice lacking AE2 should abolish the EOG. Because *AE2* KO mice do not survive beyond weaning, all experiments used young mice (13–16 days postnatal). In the other EOG experiments, mice were from 45 to 176 days old (as stated in the figure legends).

The EOG in *AE2* KO mice was normal. The mean amplitude was $510 \pm 68\ \mu V$ ($n = 7$) in the KO mice and $529 \pm 76\ \mu V$ ($n = 6$) in the *AE2* WT mice. Bumetanide (50 μM) decreased the EOG within 5 min of its application (Fig. 5*C*). There was no difference in percentage reduction between the WT and *AE2* KO epithelia ($P < 0.06$). When both data sets (WT and KO) were combined, the percentage reduction by bumetanide was 36%. This decrease is highly significant ($P < 0.0001$). Thus, bumetanide reduces the EOG amplitude but does not abolish the response even in *AE2* KO mice. These results do not support the hypothesis that AE2 plays a major role in Cl^- accumulation. However, it is possible that AE2 is expressed at lower levels in young mice than in adults.

Application of blockers to both surfaces of the mucosa

With three possible transport mechanisms blocked (Fig. 4), there remained a significant EOG response that was sensitive to niflumic acid. In other words, some Cl^- accumulation persisted even in the presence of the three blockers. It is possible that the block was incomplete because the reagents were only able to access Cl^- transport sites on the apical surface of the epithelium. To test this possibility, we developed a preparation in which both the apical and basal surfaces of the mucosa were perfused. The mucosa covering the nasal septum of a WT mouse was removed and mounted on a nylon mesh. The perfusion tube was placed so that both surfaces were perfused (see Methods). The mean EOG amplitude measured in this preparation ($629 \pm 54\ \mu V$, $n = 17$) was smaller that in the standard preparation ($913 \pm 96\ \mu V$, $n = 20$; $P < 0.02$).

In the doubly perfused mucosae, bumetanide (50 μM) reduced the EOG amplitude by 48%, while DIDS (500 μM) reduced it by 57% (Fig. 5*D*). There was no difference between the reductions produced by bumetanide and by DIDS. Combination of both drugs reduced the response by 63%. All of the reductions were highly significant ($P < 0.0001$). Differences between either drug alone and the combination were significant ($P < 0.05$, bumetanide; $P < 0.01$, DIDS). The effects of bumetanide and DIDS were not simply additive. In general, quantitatively predicting the additivity of multiple blockers requires a knowledge of the ionic gradients and the relative fluxes of the underlying transporters.

In the doubly perfused mucosae, niflumic acid (300 μM) was applied following the treatments with bumetanide and/or DIDS. Niflumic acid reduced the response amplitude by $87 \pm 3\%$ (compared with the mean control value) after 5 min of exposure and by $94 \pm 3\%$ after 10 min ($n = 3$ for bumetanide; $n = 6$ for DIDS; $n = 5$ for bumetanide plus DIDS). These results indicate that an odour-induced Cl^- current persists even following perfusion of both sides of the membrane with DIDS and bumetanide.

Discussion

When vertebrate ORNs depolarize in response to an odour stimulus, most of the current is due to an efflux of Cl^-. Presumably, Cl^- transport proteins allow the neuron to accumulate Cl^- at rest to a concentration that is above electrochemical equilibrium. One such transporter, NKCC1, clearly contributes to this process (Kaneko *et al.* 2004; Reisert *et al.* 2005; Nickell *et al.* 2006). However, substantial Cl^- accumulation persists even in mice lacking NKCC1 (Nickell *et al.* 2006). To identify the other Cl^- uptake mechanisms involved, we have taken two approaches. First, we used RT-PCR to screen nasal tissue containing olfactory mucosa for the mRNA of Cl^- transporters. Second, we characterized the pharmacological properties of neuronal Cl^- accumulation in intact olfactory epithelium.

Using RT-PCR, mRNA transcripts for 20 of the 21 Cl^- transporters were detected in nasal tissue that contained olfactory mucosa, and the identities of the PCR products were confirmed by sequencing. The remaining transporter, *DRA*, was detected as a weak band; sequencing of that band was not attempted. The *AE1* variant, *eAE1*, was detected in nasal tissue; *kAE1* was not detected. The *eAE1* signal may have resulted solely from the presence of erythrocytes, which strongly express *eAE1* (Alper *et al.* 2002).

We found a *KCC4* mRNA splice variant in nasal tissue that was not present when we sequenced the PCR product from kidney. An examination of the *KCC4* genomic sequence (NM_011390) showed that the extra 15-base sequence is present in the intron that precedes exon 23. In addition, the extra exon was bordered by the 'AG' and 'GT' splice signals that are nearly always found at the end and beginning of introns, respectively (Smith & Valcárcel, 2000). The five extra amino acids (EWGNL) in the nasal KCC4 are in the putative cytoplasmic carboxyl tail of the protein. When the amino acid sequences of KCC4 and KCC2 are aligned, the five extra residues in the nasal KCC4 line up with and closely match five amino acids (EWENL) in KCC2. For *NCBE*, we detected a new mRNA splice variant upon sequencing the PCR product from nasal tissue. The nasal *NCBE* is missing exon 25 found in the published sequence (NM_033552).

Our RT-PCR results are consistent with previous studies, with two exceptions (*KCC2* and *NKCC2*). In contrast to the RT-PCR findings of Kaneko *et al.* (2004) in rat, we did detect *KCC2* in mouse nasal tissue. Our detection of *NKCC2* is surprising, since *NKCC2* is known as a kidney-specific gene (Russell, 2000). In a microarray screen of 62 mouse tissues including 'olfactory epithelium', *NKCC2* was detected only in kidney (Su *et al.* 2004). Using RT-PCR, Kaneko *et al.* (2004) and Reisert *et al.* (2005) did not detect *NKCC2* in olfactory tissue from rat and mouse, respectively. Contamination as an alternative explanation is significantly weakened by the precautions and 'no-transcript' control described in Methods and our inability to detect another kidney gene, *kAE1,* in the same two nasal samples that expressed *NKCC2*. As an additional test, nasal tissue was acquired and processed in conjunction with a blank sample through the RNA extraction, DNase treatment and RT-PCR reaction. This nasal sample was positive for *NKCC2,* as shown by sequencing, while the control was negative (data not shown).

Our other RT-PCR findings are in accord with previous reports. Using RT-PCR, Kaneko *et al.* (2004) detected *NKCC1*, *NCC,* and *KCC1* in rat olfactory tissue and Reisert *et al.* (2005) detected *NKCC1* in mouse olfactory tissue, as did we in mouse. By microarray analysis of adult mouse olfactory mucosa, Shetty *et al.* (2005) found mRNA expression of *AE2*, *AE3*, *NKCC1* and *KCC4*, as did we by RT-PCR. In that study, other Cl^- transporters were either not tested or gave no signal on the arrays. In microarray analysis of a preparation highly enriched in mature ORNs (taken from postnatal day 11 mice), McClintock and coworkers detected expression of *AE2*, *NKCC1*, *KCC2*, *KCC3*, *KCC4*, *CIP1* and *PAT1*, while *AE1* and *SUT2* were detected primarily in a preparation of olfactory mucosa depleted of mature ORNs (T. S. McClintock, personal communication and Sammeta *et al.* 2007). The other Cl^- transporters were either not represented on the array or had signals too low to be interpreted. Using RT-PCR, we detected the same nine transporters in nasal tissue.

Screening by RT-PCR in nasal tissue did not eliminate many of the candidate Cl^- transporters. Several cell types contribute mRNA to the nasal sample (e.g. ORNs, respiratory epithelial cells, glandular cells, muscle cells) and this may explain the large number of Cl^- transporters detected. Ultimately, single-cell RT-PCR or *in situ* hybridization will be needed to determine which transporters are expressed in ORNs, and subsequent immunostaining could determine subcellular localizations.

An independent approach is to characterize Cl^- accumulation in ORNs using pharmacological methods and genetic ablation of specific transporters. As described in the introduction, the known Cl^- transporters can be grouped into four pharmacological classes. The relative contributions of these classes were estimated using an indirect assay of neuronal Cl^- accumulation, the electro-olfactogram (EOG).

The first pharmacological class of Cl^- transporters consists of NKCC1 and NKCC2. It is established that NKCC1 contributes to Cl^- accumulation in ORNs (Kaneko *et al.* 2004; Reisert *et al.* 2005; Nickell *et al.* 2006). Block of NKCC1 cotransport by bumetanide (Figs 3 and 5*D*) and genetic knockout of NKCC1 (Nickell *et al.* 2006) have similar effects on the EOG. Both reduce the EOG amplitude but leave a substantial response. This residual response is largely blocked by niflumic acid, which indicates that the ORNs accumulate Cl^- even in the absence of NKCC function (Nickell *et al.* 2006). The fact that the NKCC inhibitor, bumetanide, did not inhibit the EOG in *NKCC1* KO mice (Fig. 3) suggests that any NKCC2 present in nasal tissue contributes little to the olfactory response. Taken together, these results confirm that NKCC1 is an important factor in Cl^- accumulation but also demonstrate that, in intact epithelium, other transporters or mechanisms are important and can compensate for the absence of NKCC1.

The second pharmacological class of Cl^- transporters has a single member, NCC. RT-PCR indicates that *NCC* is expressed in nasal tissue (Kaneko *et al.* 2004; and Fig. 2*B*), but inhibition of NCC by hydrochlorothiazide only slightly reduced the EOG (Fig. 5*A*). Thus, the unidentified Cl^- uptake mechanisms may be accounted for by the third or fourth pharmacological classes of Cl^- transporters, i.e. KCC and the Cl^-/HCO_3^- exchangers. Cl^-/HCO_3^- exchangers are known to mediate Cl^- uptake. KCC cotransporters most often mediate outward K^+ and Cl^- fluxes, but they may operate in the reverse mode under certain conditions, as discussed below. Our pharmacological results support the involvement of KCC or a Cl^-/HCO_3^- exchanger in Cl^- uptake. DIDS, which blocks many transporters in these two classes, reduced the EOG amplitude significantly (Fig. 5*B, D*). This reduction was clear even when NKCC1 function was eliminated by genetic ablation (Fig. 5*B*) or with bumetanide (Fig. 5*D*). Thus, there is a mechanism of neuronal Cl^- uptake that is DIDS sensitive and clearly distinct from NKCC1. Studies of Cl^- transporters in other systems have found that cells often express both NKCC1 and a Cl^-/HCO_3^- exchanger, each serving to accumulate Cl^- (Evans *et al.* 2000; Grubb *et al.* 2000; Walker *et al.* 2002). Having two methods of Cl^- accumulation available allows this function to persist despite changes in the ionic environment. The molecular identity of the DIDS-sensitive olfactory Cl^- transporter is not yet known. The common anion exchanger AE2 is an unlikely candidate, since the EOG was found to have a normal amplitude in *AE2* KO mouse pups.

Block by DIDS does not discriminate between Cl^-/HCO_3^- exchangers and KCC cotransporters. KCC is most often assumed to cause extrusion of cytoplasmic Cl^- rather than its accumulation. It seems likely that ORNs do

have a mechanism for Cl^- extrusion. When an effective transport blocker was applied to the epithelium, the EOG was reduced within 5 min. This implies a rapid reduction of neuronal cytoplasmic Cl^-. Whether this Cl^- extrusion is via a transporter or a leak channel is unknown.

Unlike NKCC and NCC, KCC has a driving force that is usually near equilibrium (Payne *et al.* 2003; Gamba, 2005). In some circumstances, the neuron-specific form KCC2 has been shown to contribute to accumulation of cytoplasmic Cl^- (DeFazio *et al.* 2000; Kakazu *et al.* 2000). This is favoured when external K^+ is elevated or internal Cl^- is low. Ionic concentrations measured at the dendritic ending of rat ORNs (Reuter *et al.* 1998; Kaneko *et al.* 2004) would support extrusion of Cl^- by KCC. During the odour response, though, it is predicted that both K^+ and Cl^- will be greatly depleted from the ciliary lumen (Lindemann, 2001). At that point any KCC in or near the cilia might serve to recover cytoplasmic Cl^- lost during the odour response. When assayed by immunohistochemistry, some mouse ORNs show intense dendritic labelling for KCC2 (Schannen & Delay, 2005).

In no case were we able to completely eliminate the Cl^- component of the EOG by blocking and/or ablating Cl^- transporters. For this purpose we simultaneously blocked NKCC1, NCC and DIDS-sensitive transporters in WT mice (Fig. 4); blocked NCC (Fig. 5*A*) or DIDS-sensitive transporters (Fig. 5*B*) in *NKCC1* KO mice; and blocked NKCC1 in *AE2* KO mice (Fig. 5*C*). It was expected that the small cationic component of the transduction current would remain but not the Cl^- component. Niflumic acid blocks the Cl^- component of the EOG. Block of the remaining EOG by niflumic acid indicates that the ORNs accumulated Cl^- to some extent under all of the conditions tested. Ensuring that the blockers reached both surfaces of the mucosa (Fig. 5*D*) did not modify this conclusion. It remains possible that there are mechanisms of Cl^- uptake not affected by the blockers at the concentrations we tested. In general, we used the blockers at concentrations typical of those reported in other studies (see the references in the introduction). Dose–response properties for blockers of many Cl^- transporters have been determined but not in olfactory epithelium. The pharmacologies of several recently discovered Cl^- transporters (e.g. Slc26a11) are not well described in any system.

To assess neuronal Cl^- uptake, we measured the component of the EOG that was blocked by niflumic acid. The EOG is believed to arise primarily from the receptor potentials of the ORNs with little direct contribution from other epithelial cells (Ottoson, 1956; Scott & Scott-Johnson, 2002). Several studies support this view. Transection of the olfactory nerve reduces the number of ORNs, and the amplitude of the EOG decreases in parallel (Takagi & Yajima, 1965). Eliminating the primary neuronal odour transduction pathway is sufficient to virtually abolish the EOG. This has been demonstrated in mice lacking the CNGA2 subunit of the CNG channel (Brunet *et al.* 1996) or the type III adenylate cyclase (Wong *et al.* 2000). These transduction proteins are expressed in ORNs but not in other cells of the olfactory epithelium (Bakalyar & Reed, 1990; Dhallan *et al.* 1990).

It is important to consider whether any of the blockers used might have reduced the EOG not by reducing Cl^- transport but by directly blocking the transduction channels. DIDS, for example, is known to block some Cl^- channels. Effects of bumetanide and DIDS on the two types of transduction channel were determined in frog, where recording from single olfactory cilia is possible. At the concentrations used in this study, extracellular bumetanide and DIDS reduced the ciliary Cl^- conductance by 7% and 13%, respectively; they had no effect on the CNG conductance. By contrast, perfusion of both sides of the epithelium with either blocker produced a much greater reduction of the EOG amplitude (48% with bumetanide, 57% with DIDS, Fig. 5*D*). These decreases are much greater than the direct effects of the blockers on the membrane channels.

The cellular locations of the Cl^- transporters cannot be inferred from our work. Perfusing the mucosal (apical) surface of the epithelium with bumetanide reduced the EOG amplitude by 32% to 36% (Figs 3 and 5*C*). This suggests that NKCC1 functions apically but not necessarily in the cilia; perfusion of the apical surface affects the cytoplasmic Cl^- concentration in at least the most apical extent of the dendrite (Kaneko *et al.* 2004). It is possible that the dendritic endings, like some other dendrites (Gavrikov *et al.* 2006) and presynaptic terminals (Price & Trussell, 2006), may regulate cytoplasmic Cl^- independently of the rest of the neuron. However, when both surfaces of the epithelium were perfused with bumetanide, the EOG amplitude was more effectively reduced (48%, Fig. 5*D*). This greater reduction suggests that basolateral NKCC1 may also influence $[Cl^-]$ even in the sensory ending. The 48% reduction on double perfusion is nearly as great as the reduction from genetic ablation of NKCC1 (57%). It is likely, then, that double perfusion with 50 μM bumetanide provides a nearly complete block of NKCC1 activity.

The present results in intact epithelium differ substantially from those determined in isolated ORNs (Reisert *et al.* 2005). In isolated neurons, NKCC1 appears to be necessary and sufficient for accumulation of Cl^-. Accumulation in intact tissue is more robust and persists even when NKCC1 is blocked or genetically ablated. Although the precise reason for this disparity is not understood, there are obvious differences between the two preparations. Isolated neurons allow better control of the extracellular environment and odour delivery. However, the intact epithelium better preserves the several extracellular compartments present *in vivo*. In particular, the sustentacular cells probably help to regulate the interstitial and apical compartments. It is possible that they

also contribute more directly to the EOG, but evidence discussed above indicates that the EOG arises primarily from the olfactory receptor neurons. *In vivo*, several transport systems may be interlinked to simultaneously regulate not only the intraneuronal Cl^-, but also the volume, pH and resting potential of the ORN. Thus, generation of an electrochemical gradient may be substantially more complex *in vivo* than in isolated ORNs.

In conclusion, Cl^- accumulation in ORNs involves at least two transporters, NKCC1 and a DIDS-sensitive transporter. The molecular identity of the second is not known, but it is likely to be a KCC cotransporter or a Cl^-/HCO_3^- exchanger.

References

Alper SL, Darman RB, Chernova MN & Dahl NK (2002). The AE family of Cl^-/HCO_3^- exchangers. *J Nephrol* **15** (Suppl. 5), S41–S53.

Altschul SF, Madden TL, Schäffer AA, Zhang J, Zhang Z, Miller W & Lipman DJ (1997). Gapped BLAST and PSI-BLAST: a new generation of protein database search programs. *Nucl Acids Res* **25**, 3389–3402.

Bakalyar HA & Reed RR (1990). Identification of a specialized adenylyl cyclase that may mediate odorant detection. *Science* **250**, 1403–1406.

Boccaccio A & Menini A (2007). Temporal development of CNG and Ca^{2+}-activated Cl^- currents in isolated mouse olfactory sensory neurons. *J Neurophysiol* **98**, 153–160.

Brunet LJ, Gold GH & Ngai J (1996). General anosmia caused by a targeted disruption of the mouse olfactory cyclic nucleotide-gated cation channel. *Neuron* **17**, 681–693.

DeFazio RA, Keros S, Quick MW & Hablitz JJ (2000). Potassium-coupled chloride cotransport controls intracellular chloride in rat neocortical pyramidal neurons. *J Neurosci* **20**, 8069–8076.

Delpire E & Lauf PK (1992). Kinetics of DIDS inhibition of swelling-activated K-Cl cotransport in low K sheep erythrocytes. *J Membr Biol* **126**, 89–96.

Dhallan RS, Yau K-W, Schrader KA & Reed RR (1990). Primary structure and functional expression of a cyclic nucleotide-activated channel from olfactory neurons. *Nature* **347**, 184–187.

Dossena S, Vezzoli V, Cerutti N, Bazzini C, Tosco M, Sironi C *et al*. (2006). Functional characterization of wild-type and a mutated form of SLC26A4 identified in a patient with Pendred syndrome. *Cell Physiol Biochem* **17**, 245–256.

Evans RL, Park K, Turner RJ, Watson GE, Nguyen HV, Dennett MR *et al*. (2000). Severe impairment of salivation in $Na^+/K^+/2Cl^-$ cotransporter (NKCC1) -deficient mice. *J Biol Chem* **275**, 26720–26726.

Farbman AI (1992). *Cell Biology of Olfaction*, pp. 25, 46, 49. Cambridge University Press, Cambridge.

Flagella M, Clarke LL, Miller ML, Erway LC, Giannella RA, Andringa A *et al*. (1999). Mice lacking the basolateral Na-K-2Cl cotransporter have impaired epithelial chloride secretion and are profoundly deaf. *J Biol Chem* **274**, 26946–26955.

Frings S (2001). Chemoelectrical signal transduction in olfactory sensory neurons of air-breathing vertebrates. *Cell Mol Life Sci* **58**, 510–519.

Gamba G (2005). Molecular physiology and pathophysiology of electroneutral cation-chloride cotransporters. *Physiol Rev* **85**, 423–493.

Gavrikov KE, Nilson JE, Dmitriev AV, Zucker CL & Mangel SC (2006). Dendritic compartmentalization of chloride cotransporters underlies directional responses of starburst amacrine cells in retina. *Proc Natl Acad Sci U S A* **103**, 18793–18798.

Gawenis LR, Ledoussal C, Judd LM, Prasad V, Alper SL, Stuart-Tilley A *et al*. (2004). Mice with a targeted disruption of the AE2 Cl^-/HCO_3^- exchanger are achlorhydric. *J Biol Chem* **279**, 30531–30539.

Gesteland RC, Lettvin JY & Pitts WH (1965). Chemical transmission in the nose of the frog. *J Physiol* **181**, 525–559.

Gesteland RC & Sigwart CD (1977). Olfactory receptor units – a mammalian preparation. *Brain Res* **133**, 144–149.

Greeley T, Shumaker H, Wang Z, Schweinfest CW & Soleimani M (2001). Downregulated in adenoma and putative anion transporter are regulated by CFTR in cultured pancreatic duct cells. *Am J Physiol Gastrointest Liver Physiol* **281**, G1301–G1308.

Grubb BR, Lee E, Pace AJ, Koller BH & Boucher RC (2000). Intestinal ion transport in NKCC1-deficient mice. *Am J Physiol Gastrointest Liver Physiol* **279**, G707–G718.

Hebert SC, Mount DB & Gamba G (2004). Molecular physiology of cation-coupled Cl^- cotransport: the SLC12 family. *Pflugers Arch* **447**, 580–593.

Kakazu Y, Uchida S, Nakagawa T, Akaike N & Nabekura J (2000). Reversibility and cation selectivity of the K^+-Cl^- cotransport in rat central neurons. *J Neurophysiol* **84**, 281–288.

Kaneko H, Putzier I, Frings S, Kaupp UB & Gensch T (2004). Chloride accumulation in mammalian olfactory sensory neurons. *J Neurosci* **24**, 7931–7938.

Kietz D, Bartel D, Lepke S & Passow H (1991). pH-dependence of inhibition by H_2DIDS of mouse erythroid band 3-mediated Cl^- transport in *Xenopus* oocytes. The effect of oligonucleotide-directed replacement of Lys-558 by an Asn residue. *Biochim Biophys Acta* **1064**, 81–88.

Kleene SJ (1993). Origin of the chloride current in olfactory transduction. *Neuron* **11**, 123–132.

Kleene SJ & Pun RYK (1996). Persistence of the olfactory receptor current in a wide variety of extracellular environments. *J Neurophysiol* **75**, 1386–1391.

Ko SBH, Luo X, Hagar H, Rojek A, Choi JY, Licht C, Suzuki M, Muallem S, Nielsen S & Ishibashi K (2002). AE4 is a DIDS-sensitive Cl^-/HCO_3^- exchanger in the basolateral membrane of the renal CCD and the SMG duct. *Am J Physiol Cell Physiol* **283**, C1206–C1218.

Kurahashi T & Yau K-W (1993). Co-existence of cationic and chloride components in odorant-induced current of vertebrate olfactory receptor cells. *Nature* **363**, 71–74.

Lee BS, Gunn RB & Kopito RR (1991). Functional differences among nonerythroid anion exchangers expressed in a transfected human cell line. *J Biol Chem* **266**, 11448–11454.

Lindemann B (2001). Predicted profiles of ion concentrations in olfactory cilia in the steady state. *Biophys J* **80**, 1712–1721.

Lohi H, Kujala M, Mäkelä S, Lehtonen E, Kestilä M, Saarialho-Kere U, Markovich D & Kere J (2002). Functional characterization of three novel tissue-specific anion exchanger SLC26A7, -A8, and -A9. *J Biol Chem* **277**, 14246–14254.

Lowe G & Gold GH (1993). Nonlinear amplification by calcium-dependent chloride channels in olfactory receptor cells. *Nature* **266**, 283–286.

Melvin JE, Park K, Richardson L, Schultheis PJ & Shull GE (1999). Mouse down-regulated in adenoma (DRA) is an intestinal Cl^-/HCO_3^- exchanger and is up-regulated in colon of mice lacking the NHE3 Na^+/H^+ exchanger. *J Biol Chem* **274**, 22855–22861.

Mercado A, Song L, Vázquez N, Mount DB & Gamba G (2000). Functional comparison of the K^+-Cl^- cotransporters KCC1 and KCC4. *J Biol Chem* **275**, 30326–30334.

Mount DB & Romero MF (2004). The SLC26 gene family of multifunctional anion exchangers. *Pflugers Arch* **447**, 710–721.

Nakamura T & Gold GH (1987). A cyclic nucleotide-gated conductance in olfactory receptor cilia. *Nature* **325**, 442–444.

Nickell WT, Kleene NK, Gesteland RC & Kleene SJ (2006). Neuronal chloride accumulation in olfactory epithelium of mice lacking NKCC1. *J Neurophysiol* **95**, 2003–2006.

Ottoson D (1956). Analysis of the electrical activity of the olfactory epithelium. *Acta Physiol Scand Suppl* **122**, 1–83.

Payne JA (1997). Functional characterization of the neuronal-specific K-Cl cotransporter: implications for $[K^+]_o$ regulation. *Am J Physiol Cell Physiol* **273**, C1516–C1525.

Payne JA, Rivera C, Voipio J & Kaila K (2003). Cation-chloride co-transporters in neuronal communication, development and trauma. *Trends Neurosci* **26**, 199–206.

Petrovic S, Barone S, Xu J, Conforti L, Ma L, Kujala M, Kere J & Soleimani M (2004). SLC26A7: a basolateral Cl^-/HCO_3^- exchanger specific to intercalated cells of the outer medullary collecting duct. *Am J Physiol Renal Physiol* **286**, F161–F169.

Petrovic S, Xie J, Barone S, Seidler U, Alper S, Lohi H, Kere J & Soleimani M (2003). Identification of a basolateral Cl^-/HCO_3^- exchanger specific to gastric parietal cells. *Am J Physiol Gastrointest Liver Physiol* **284**, G1093–G1103.

Price GD & Trussell LO (2006). Estimate of the chloride concentration in a central glutamatergic terminal: a gramicidin perforated-patch study on the calyx of Held. *J Neurosci* **26**, 11432–11436.

Reisert J, Lai J, Yau K-W & Bradley J (2005). Mechanism of the excitatory Cl^- response in mouse olfactory receptor neurons. *Neuron* **45**, 553–561.

Ressler KJ, Sullivan SL & Buck LB (1993). A zonal organization of odorant receptor gene expression in the olfactory epithelium. *Cell* **73**, 597–609.

Reuter D, Zierold K, Schröder WH & Frings S (1998). A depolarizing chloride current contributes to chemoelectrical transduction in olfactory sensory neurons *in situ*. *J Neurosci* **18**, 6623–6630.

Romero MF, Fulton CM & Boron WF (2004). The SLC4 family of HCO_3^- transporters. *Pflugers Arch* **447**, 495–509.

Rozen S & Skaletsky HJ (2000). Primer3 on the WWW for general users and for biologist programmers. In *Bioinformatics Methods and Protocols: Methods in Molecular Biology*, ed Krawetz S & Misener S, pp. 365–386. Humana Press, Totowa, NJ.

Russell JM (2000). Sodium-potassium-chloride cotransport. *Physiol Rev* **80**, 212–276.

Sammeta N, Yu TT, Bose SC & McClintock TS (2007). Mouse olfactory sensory neurons express 10,000 genes. *J Comp Neurol* **502**, 1138–1156.

Schannen AP & Delay R (2005). Expression of Cl^- cotransporters in mouse olfactory neurons [Abstract]. *Chem Senses* **30**, A80; http://chemse.oxfordjournals.org/cgi/reprint/30/3/A1

Schild D & Restrepo D (1998). Transduction mechanisms in vertebrate olfactory receptor cells. *Physiol Rev* **78**, 429–466.

Scott JW & Scott-Johnson PE (2002). The electroolfactogram: a review of its history and uses. *Microsc Res Tech* **58**, 152–160.

Shetty RS, Bose SC, Nickell MD, McIntyre JC, Hardin DH, Harris AM & McClintock TS (2005). Transcriptional changes during neuronal death and replacement in the olfactory epithelium. *Mol Cell Neurosci* **30**, 583–600.

Smith CWJ & Valcárcel J (2000). Alternative pre-mRNA splicing: the logic of combinatorial control. *Trends Biochem Sci* **25**, 381–388.

Soleimani M, Greeley T, Petrovic S, Wang Z, Amlal H, Kopp P & Burnham C (2001). Pendrin: an apical $Cl^-/OH^-/HCO_3^-$ exchanger in the kidney cortex. *Am J Physiol Renal Physiol* **280**, F356–F364.

Soleimani M & Xu J (2006). SLC26 chloride/base exchangers in the kidney in health and disease. *Semin Nephrol* **26**, 375–385.

Spehr M, Kelliher KR, Li X-H, Boehm T, Leinders-Zufall T & Zufall F (2006). Essential role of the main olfactory system in social recognition of major histocompatibility complex peptide ligands. *J Neurosci* **26**, 1961–1970.

Sterling D & Casey JR (2002). Bicarbonate transport proteins. *Biochem Cell Biol* **80**, 483–497.

Stokes JB (1984). Sodium chloride absorption by the urinary bladder of the winter flounder. *J Clin Invest* **74**, 7–16.

Su AI, Wiltshire T, Batalov S, Lapp H, Ching K, Block D *et al*. (2004). A gene atlas of the mouse and human protein-encoding transcriptomes. *Proc Natl Acad Sci U S A* **101**, 6062–6067.

Takagi SF & Yajima T (1965). Electrical activity and histological change in the degenerating olfactory epithelium. *J Gen Physiol* **48**, 559–569.

Tsuganezawa H, Kobayashi K, Iyori M, Araki T, Koizumi A, Watanabe S *et al*. (2001). A new member of the HCO_3^- transporter superfamily is an apical anion exchanger of β-intercalated cells in the kidney. *J Biol Chem* **276**, 8180–8189.

Vincourt J-B, Jullien D, Amalric F & Girard J-P (2003). Molecular and functional characterization of SLC26A11, a sodium-independent sulfate transporter from high endothelial venules. *FASEB J* **17**, 890–892.

Walker NM, Flagella M, Gawenis LR, Shull GE & Clarke LL (2002). An alternate pathway of cAMP-stimulated Cl secretion across the NKCC1-null murine duodenum. *Gastroenterology* **123**, 531–541.

Wang Z, Petrovic S, Mann E & Soleimani M (2002). Identification of an apical Cl^-/HCO_3^- exchanger in the small intestine. *Am J Physiol Gastrointest Liver Physiol* **282**, G573–G579.

Wang Z, Sindreu CB, Li V, Nudelman A, Chan GC-K & Storm DR (2006). Pheromone detection in male mice depends on signaling through the type 3 adenylyl cyclase in the main olfactory epithelium. *J Neurosci* **26**, 7375–7379.

Wang CZ, Yano H, Nagashima K & Seino S (2000). The Na^+-driven Cl^-/HCO_3^- exchanger. *J Biol Chem* **275**, 35486–35490.

Wheat VJ, Shumaker H, Burnham C, Shull GE, Yankaskas JR & Soleimani M (2000). CFTR induces the expression of DRA along with Cl^-/HCO_3^- exchange activity in tracheal epithelial cells. *Am J Physiol Cell Physiol* **279**, C62–C71.

Wong ST, Trinh K, Hacker B, Chan GCK, Lowe G, Gaggar A, Xia Z, Gold GH & Storm DR (2000). Disruption of the type III adenylyl cyclase gene leads to peripheral and behavioral anosmia in transgenic mice. *Neuron* **27**, 487–497.

Xu J, Barone S, Petrovic S, Wang Z, Seidler U, Riederer B, Ramaswamy K, Dudeja PK, Shull GE & Soleimani M (2003). Identification of an apical Cl^-/HCO_3^- exchanger in gastric surface mucous and duodenal villus cells. *Am J Physiol Gastrointest Liver Physiol* **285**, G1225–G1234.

Xu J, Henriksnäs J, Barone S, Witte D, Shull GE, Forte JG, Holm L & Soleimani M (2005). SLC26A9 is expressed in gastric surface epithelial cells, mediates Cl^-/HCO_3^- exchange, and is inhibited by NH_4^+. *Am J Physiol Cell Physiol* **289**, C493–C505.

Zhainazarov AB & Ache BW (1995). Odor-induced currents in *Xenopus* olfactory receptor cells measured with perforated-patch recording. *J Neurophysiol* **74**, 479–483.

Acknowledgements

We are grateful to Gary Shull, Lara Gawenis and Emily Bradford for KO mice and many helpful discussions; to Gary Shull for reading the manuscript; to Manoocher Soleimani for advice and primer sequences; to Jianhua Zhang and Linda Parysek for advice on RT-PCR and splice variants; to James Deddens for statistical consultation; and to Tim McClintock for personal communication of unpublished data. This work was supported in part by research grant R01 DC00926 from the National Institute on Deafness and Other Communicative Disorders, National Institutes of Health; and by the College of Medicine Dean's Bridge Funding Program and the University Research Council of the University of Cincinnati.

Supplemental material

Online supplemental material for this paper can be accessed at:
http://jp.physoc.org/cgi/content/full/jphysiol.2007.129601/DC1

and

http://www.blackwell-synergy.com/doi/suppl/10.1113/jphysiol.2007.129601